

## Nonheme Manganese-Catalyzed Asymmetric Oxidation. A Lewis Acid Activation versus Oxygen Rebound Mechanism: Evidence for the “Third Oxidant”

Roman V. Ottenbacher, Konstantin P. Bryliakov,\* and Evgenii P. Talsi

*Novosibirsk State University, Ul. Pirogova 2, Novosibirsk 630090, Russian Federation, and Boreskov Institute of Catalysis, Siberian Branch of the Russian Academy of Sciences, Pr. Lavrentieva 5, Novosibirsk 630090, Russian Federation*

Received June 29, 2010

The catalytic properties of a series of chiral nonheme aminopyridinylmanganese(II) complexes  $[\text{LMn}^{\text{II}}(\text{OTf})_2]$  were investigated. The above complexes were found to efficiently catalyze enantioselective olefin oxidation to the corresponding epoxides with different oxidants (peroxycarboxylic acids, alkyl hydroperoxides, iodosylarenes, etc.) with high conversions and selectivities (up to 100%) and enantiomeric excesses (up to 79%). The effect of the ligand structure on the catalytic performance was probed. Epoxidation enantioselectivities were found to be strongly dependent on the structure of the oxidants (performic, peracetic, and *m*-chloroperbenzoic acids; *tert*-butyl and cumyl hydroperoxides; iodosylbenzene and iodosylmesitylene), thus bearing evidence that the terminal oxidant molecule is incorporated in the structure of the oxygen-transferring intermediates. High-valence electron-paramagnetic-resonance-active manganese complexes  $[\text{LMn}^{\text{IV}}=\text{O}]^{2+}$  and  $[\text{LMn}^{\text{IV}}(\mu\text{-O})_2\text{Mn}^{\text{III}}\text{L}]^{3+}$  were detected upon interaction of the starting catalyst with the oxidants. The high-valence complexes did not epoxidize styrene and could themselves only contribute to minor olefin oxidation sideways. However, the oxomanganese(IV) species were found to perform the Lewis acid activation of the acyl and alkyl hydroperoxides or iodosylarenes to form the new type of oxidant [oxomanganese(IV) complex with a terminal oxidant], with the latter accounting for the predominant enantioselective epoxidation pathway in the nonheme manganese-catalyzed olefin epoxidations.

### Introduction

Oil and gas hydrocarbons are rather inert compounds themselves and require functionalization (mainly oxygenation) prior to use as chemical stuff.<sup>1a</sup> The selective and sustainable chemical oxidative functionalization of hydrocarbons is still challenging, while natural oxygenases catalyze such processes smoothly at ambient conditions.<sup>1</sup> There have been considerable efforts directed to the search for the synthetic prototypes of natural metalloenzymes capable of modeling the structures and functions of the latter.<sup>1a,d,e</sup> This *biomimetic catalytic oxidation* area has been continuously expanding and periodically reviewed in recent years, with particular focus on iron-based catalysts,<sup>1a–g</sup> however, other metal-based biomimetic oxidation catalysts are considered as well.<sup>1h–j</sup>

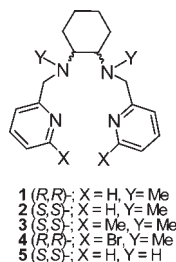
Manganese complexes have been attracting significant attention as selective and stereoselective hydrocarbon oxidation catalysts since the mid-1980s,<sup>2a,b</sup> especially after breakthroughs of the Jacobsen and Katsuki groups resulting in the development of effective and stereoselective manganese(III) salen catalysts for the catalytic asymmetric epoxidation of unfunctionalized olefins.<sup>2c–f</sup> Remarkably, the Katsuki–Jacobsen  $\text{Mn}^{\text{III}}(\text{salen})$  complexes were reported to catalyze asymmetric olefin epoxidation with iodosylarenes, aqueous bleach, and *m*-chloroperbenzoic acid (*m*-CPBA).<sup>2c–f</sup> Despite extensive discussions, the mechanism of catalytic action of manganese salen complexes remained essentially hypothetical (details of these discussions can be found in circumstantial reviews of Gilheany and co-workers<sup>3</sup>). Importantly, electron paramagnetic resonance (EPR) spectroscopy was successfully

\*To whom correspondence should be addressed. E-mail: bryliako@catalysis.ru. Fax: +7 383 3308056.

(1) (a) Steinman, A. A. *Russ. Chem. Rev.* 2008, 77, 945–966. (b) *Active Oxygen in Biochemistry*; Valentine, J. S., Foote, C. S., Greenberg, A., Liebmann, J. F., Eds.; Chapman and Hall: London, 1995. (c) Shilov, A. E. *Metal Complexes in Biomimetic Chemical Reactions*; CRC Press: New York, 1997. (d) Costas, M.; Mehn, M. P.; Jensen, M. P.; Que, L., Jr. *Chem. Rev.* 2004, 104, 939–986. (e) Oldenburg, P. D.; Que, L., Jr. *Catal. Today* 2006, 117, 15–21. (f) Que, L., Jr. *Acc. Chem. Res.* 2007, 40, 493–500. (g) Kryatov, S. V.; Rybak-Akimova, E. V.; Schindler, S. *Chem. Rev.* 2005, 105, 2175–2226. (h) Piera, J.; Bäckvall, J. E. *Angew. Chem., Int. Ed.* 2008, 47, 2–20. (i) Kim, E.; Chufan, E. E.; Kamaraj, K.; Karlin, K. D. *Chem. Rev.* 2004, 104, 1077–1134. (j) Enemark, J. H.; Cooney, J. J. A.; Wang, J. J.; Holm, R. H. *Chem. Rev.* 2004, 104, 1175–1200.

(2) (a) Meunier, B.; Guilmet, E.; De Carvalho, M. E.; Poilblanc, E. *J. Am. Chem. Soc.* 1984, 106, 6668–6676. (b) Srinivasan, K.; Michaud, P.; Kochi, J. K. *J. Am. Chem. Soc.* 1986, 108, 2309–2320. (c) Zhang, W.; Loebach, J. L.; Wilson, S. R.; Jacobsen, E. N. *J. Am. Chem. Soc.* 1990, 112, 2801–2803. (d) Irie, R.; Noda, K.; Ito, Y.; Matsumoto, N.; Katsuki, T. *Tetrahedron Lett.* 1990, 31, 7345–7348. (e) Jacobsen, E. N.; Zhang, W.; Loebach, J. L.; Muci, A. R.; Ecker, J. R.; Deng, L. *J. Am. Chem. Soc.* 1991, 113, 7063–7064. (f) Palucki, M.; McCormick, G. J.; Jacobsen, E. N. *Tetrahedron Lett.* 1995, 36, 5457–5460.

(3) (a) Dalton, C. T.; Ryan, K. M.; Wall, V. M.; Bousquet, C.; Gilheany, D. G. *Top. Catal.* 1998, 5, 75–91. (b) McGarrigle, E. M.; Gilheany, D. G. *Chem. Rev.* 2005, 105, 1563–1602.

**Scheme 1.** Aminopyridine Ligands Used for the Syntheses of Manganese(II) Catalysts

applied<sup>4,5a,5b</sup> to monitor the high-valence manganese intermediates in the Katsuki–Jacobsen epoxidations. The Mn<sup>III</sup>-(salen) acylperoxo complex was found to be the last detectable intermediate if one used *m*-CPBA as the oxidant, while in the system with PhIO, the O=Mn<sup>V</sup>(salen) complex<sup>5c</sup> was the main oxygen-transferring species [stocked up in the form of  $\mu$ -oxo-bridged manganese(IV) binuclear complexes].<sup>4</sup>

Despite the success of Katsuki–Jacobsen-type oxidations, manganese salen catalysts bore some intrinsic drawbacks associated with the ligand structure, in particular, the low turnover number (5–50 in most cases) due to fast catalyst degradation. In 2003, Stack and co-workers reported the aminopyridine [Mn<sup>II</sup>[(*R,R*)-bpmcn](CF<sub>3</sub>SO<sub>3</sub>)<sub>2</sub>] complex with ligand **1** (Scheme 1), which efficiently catalyzed the epoxidation of various alkenes with peracetic acid in high yields (90–99%) using down to only 0.1 mol % of the catalyst<sup>6a</sup> (although the enantioselectivity of these epoxidations was not scrutinized). A total of 19 manganese complexes were screened, revealing [Mn(**1**)(CF<sub>3</sub>SO<sub>3</sub>)<sub>2</sub>] (**Mn-1**) as the most prominent olefin epoxidation catalyst with peracetic acid.<sup>6b</sup> In 2007, oxidation of various organic substrates with peracetic acid and PhIO catalyzed by similar nonheme manganese complexes was examined.<sup>7a</sup> Costas and co-workers synthesized a novel family of pinene-derived aminopyridinylmanganese complexes that demonstrated remarkable performance and moderate stereoselectivities (4–46% ee) in the epoxidation of various substrates with peracetic acid.<sup>7b</sup>

Although the importance of understanding the nature of active intermediates can hardly be overestimated, no direct experimental evidence for the manganese aminopyridine systems has been reported so far. It has been supposed [by analogy with the Mn(salen) chemistry] that high-valence oxomanganese complexes could be involved in the crucial oxidation step<sup>6a,7b</sup> (Nam and co-workers suggested “a mechanism involving metal-based oxidants”<sup>7a</sup>). However, in many cases, the existence of alternative mechanisms for manganese- and iron-based oxidations has been established,

implicating metal oxidant complexes as the only intermediates or as the “second” and “third” active oxidants.<sup>4b,8–10</sup> In this paper, we report the results of a systematic investigation of enantioselective alkene epoxidations with a broad range of different terminal oxidants catalyzed by cationic manganese(II) complexes with aminopyridine ligands **2–4**. Importantly, an unprecedented level of asymmetric induction (up to 79% ee) has been achieved for manganese aminopyridine catalyzed epoxidations. Moreover, on the basis of the catalytic and spectroscopic (EPR and NMR) data obtained, one could reliably discriminate between the alternative oxygen-rebound and Lewis acid activation mechanisms and identify the new oxidant (a complex between the terminal oxidant and the high-valence oxomanganese complex rather similar to the “third oxidant” reported by Goldberg and co-workers<sup>10a,b</sup>) as that responsible for enantioselective epoxidation by this catalyst system.

## Results and Discussion

**Enantioselective Olefin Epoxidation.** New manganese(II) complexes with chiral ligands **2–4** were prepared and tested in the enantioselective epoxidation of various alkenes with peracetic acid. Some results are presented in Table 1. Complexes **Mn-3** and **Mn-4** (bearing either electron-donating or -withdrawing substituents in the third position) displayed rather poor activities (Table 1, entries 1–5); high conversion was observed only for the epoxidation of styrene over **Mn-2**. The latter, in contrast, led to nearly quantitative formation of epoxides of styrene and of *trans*- $\beta$ -Me-styrene and somewhat lower conversions for 1,2-dihydronaphthalene and indene (Table 1, entries 6–9).

Encouraged by the observed enantioselectivity for the epoxidation of styrene and indene with AcOOH over **Mn-2**, we attempted the epoxidation of various alkenes with other oxidants (Table 2). Both enantiomers of the catalyst (**Mn-2** and **Mn-1**) demonstrated similar yields and enantioselectivities in the epoxidation of styrene with AcOOH (entries 1 and 2). A similar result was obtained at 0 °C using only 0.5 mol % of the catalyst (entry 3). The

(8) (a) Nam, W.; Kim, H. J.; Kim, S. H.; Ho, R. Y. N.; Valentine, J. S. *Inorg. Chem.* **1996**, *35*, 1045–1049. (b) Wadhvani, P.; Mukherjee, M.; Bandyopadhyay, D. *J. Am. Chem. Soc.* **2001**, *123*, 12430–12431. (c) Yamada, T.; Imagawa, K.; Nagata, T.; Mukaiyama, T. *Bull. Chem. Soc. Jpn.* **1994**, *67*, 2248–2256. (d) Nagata, T.; Imagawa, K.; Yamada, T.; Mukaiyama, T. *Bull. Chem. Soc. Jpn.* **1995**, *68*, 1455–1465.

(9) (a) Yang, Y.; Diederich, F.; Valentine, J. S. *J. Am. Chem. Soc.* **1990**, *112*, 7826–7828. (b) Machii, K.; Watanabe, Y.; Morishima, I. *J. Am. Chem. Soc.* **1995**, *117*, 6691–6697. (c) Collman, J. P.; Chien, A. S.; Eberspacher, T. A.; Brauman, J. I. *J. Am. Chem. Soc.* **2000**, *122*, 11098–11100. (d) Nam, W.; Lim, M. H.; Lee, H. J.; Kim, C. *J. Am. Chem. Soc.* **2000**, *122*, 6641–6647. (e) Ogliaro, F.; de Visser, S. P.; Cohen, S.; Sharma, P. K.; Shaik, S. *J. Am. Chem. Soc.* **2002**, *124*, 2806–2817. (f) Collman, J. P.; Zeng, L.; Decréau, R. A. *Chem. Commun.* **2003**, 2974–2975. (g) Nam, W.; Choi, S. K.; Lim, M. H.; Rohde, J.-U.; Kim, I.; Kim, J.; Kim, C.; Que, L., Jr. *Angew. Chem., Int. Ed.* **2003**, *42*, 109–111. (h) Bryliakov, K. P.; Talsi, E. P. *Angew. Chem., Int. Ed.* **2004**, *43*, 5228–5230. (i) Bryliakov, K. P.; Talsi, E. P. *Chem.—Eur. J.* **2007**, *13*, 8045–8050. (j) Collman, J. P.; Zeng, L.; Brauman, J. I. *Inorg. Chem.* **2004**, *43*, 2672–2679. (k) Adam, W.; Roschmann, K. J.; Saha-Möller, C. R.; Seebach, D. *J. Am. Chem. Soc.* **2002**, *124*, 5068–5073.

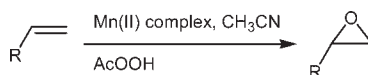
(10) (a) Wang, S. H.; Mandimutsira, B. S.; Todd, R.; Ramdhanie, B.; Fox, J. P.; Goldberg, D. P. *J. Am. Chem. Soc.* **2004**, *126*, 18–19. (b) Leeladee, P.; Goldberg, D. P. *Inorg. Chem.* **2010**, *49*, 3083–3085. (c) Yin, G.; Buchalova, M.; Danby, A. M.; Perkins, C. M.; Kitko, D.; Carter, J. D.; Scheper, W. M.; Busch, D. H. *J. Am. Chem. Soc.* **2005**, *127*, 17170–17171. (d) Zdilla, M. J.; Abu-Omar, M. M. *J. Am. Chem. Soc.* **2006**, *128*, 16971–16979.

(4) (a) Bryliakov, K. P.; Babushkin, D. E.; Talsi, E. P. *Mendeleev Commun.* **1999**, *9*, 29–31. (b) Bryliakov, K. P.; Babushkin, D. E.; Talsi, E. P. *J. Mol. Catal. A: Chem.* **2000**, *158*, 19–35.

(5) (a) Adam, W.; Mock-Knoblauch, C.; Saha-Möller, C. R.; Herderich, M. *J. Am. Chem. Soc.* **2000**, *122*, 9685–9691. (b) Campbell, K. A.; Lashley, M. R.; Wyatt, J. K.; Nantz, M. H.; David Britt, R. *J. Am. Chem. Soc.* **2001**, *123*, 5710–5719. (c) Feichtinger, D.; Plattner, D. A. *Angew. Chem., Int. Ed. Engl.* **1997**, *36*, 1718–1719.

(6) (a) Murphy, A.; Dubois, G.; Stack, T. D. P. *J. Am. Chem. Soc.* **2003**, *125*, 5250–5251. (b) Murphy, A.; Pace, A.; Stack, T. D. P. *Org. Lett.* **2004**, *6*, 3119–3122.

(7) (a) Nehru, K.; Kim, S. J.; Kim, I. Y.; Seo, M. S.; Kim, Y.; Kim, S.-J.; Kim, J.; Nam, W. *Chem. Commun.* **2007**, *41*, 4623–4625. (b) Gomez, L.; Garcia-Bosch, I.; Company, A.; Sala, X.; Fontrodona, X.; Ribas, X.; Costas, M. *J. Chem. Soc., Dalton Trans.* **2007**, *47*, 5539–5545.

Table 1. Epoxidation of Alkenes in the Presence of Complexes **Mn-3** and **Mn-4**

no.	substrate	complex	oxidant	[alkene]:[O]:[Mn]	<i>T</i> , °C	time, h	conversion, %	epoxide selectivity, %	epoxide ee, % (config)
1	styrene	<b>Mn-3</b>	AcOOH	200:250:1	0	0.25	24.8	100	11.0 ( <i>S</i> )
2	styrene	<b>Mn-3</b>	AcOOH	200:250:1	-20	2	68.0	100	9.0 ( <i>S</i> )
3	indene	<b>Mn-3</b>	AcOOH	200:250:1	0	1	16.6	90.3 <sup>a</sup>	nd <sup>b</sup>
4	( <i>E</i> )- $\beta$ -methylstyrene	<b>Mn-3</b>	AcOOH	200:250:1	0	2	19.0	100	3.0
5	styrene	<b>Mn-4</b>	AcOOH	200:250:1	-20	1	12.7	100	3.0 ( <i>S</i> )
6	styrene	<b>Mn-2</b>	AcOOH	200:250:1	-20	2	97.5	100	22.5 ( <i>R</i> )
7	indene	<b>Mn-2</b>	AcOOH	200:250:1	0	1	70.0	86.0 <sup>a</sup>	36.5 (1 <i>R</i> ,2 <i>S</i> )
8	1,2-dihydronaphthalene	<b>Mn-2</b>	AcOOH	200:250:1	0	1	86.4	92.0 <sup>a</sup>	0
9	( <i>E</i> )- $\beta$ -methylstyrene	<b>Mn-2</b>	AcOOH	200:250:1	0	2	97.8	100	0

<sup>a</sup>Side product: 1,2-diol. <sup>b</sup>nd = not determined.

Table 2. Enantioselective Epoxidation of Alkenes over **Mn-2** by Various Oxidants<sup>a</sup>

no.	substrate	complex	oxidant	[alkene]:[O]:[Mn]	<i>T</i> , °C	time, h	conversion, %	epoxide selectivity, %	epoxide ee, % (config)
1	styrene	<b>Mn-2</b>	AcOOH	100:110:1	-20	2	100	97.6 <sup>f</sup>	35.0 ( <i>R</i> )
2	styrene	<b>Mn-1</b>	AcOOH	100:110:1	-20	2	100	97.0 <sup>f</sup>	35.5 ( <i>S</i> )
3	styrene	<b>Mn-2</b>	AcOOH	200:250:1	0	0.5	94.7	100	33.0 ( <i>R</i> )
4	styrene	<b>Mn-2</b>	HCO <sub>3</sub> H	100:100:1	0	0.33	83.0	100	29.0 ( <i>R</i> )
5	styrene	<b>Mn-2</b>	<i>m</i> -CPBA	100:125:1	0	0.17	98.0	100	11.0 ( <i>R</i> )
6	styrene	<b>Mn-2</b>	<i>t</i> BuOOH	100:150:1	0	3.5	55.9	100	27.2 ( <i>R</i> )
7	styrene	<b>Mn-2<sup>e</sup></b>	<i>t</i> BuOOH	100:150:1	0	3.5	53.8	100	27.8 ( <i>R</i> )
8	styrene	<b>Mn-2</b>	CHP	100:110:1	0	2	94.5	100	18.0 ( <i>R</i> )
9	styrene	<b>Mn-2</b>	PhIO	100:110:2	0	6	84.4	100	14.5 ( <i>R</i> )
10	styrene	<b>Mn-2</b>	PhIO	100:110:2	20	0.75	72.2	100	14.5 ( <i>R</i> )
11	styrene	<b>Mn-2</b>	MesIO	100:110:2	20	0.33	58.1	100	18.0 ( <i>R</i> )
12	styrene	<b>Mn-2<sup>e</sup></b>	MesIO	100:110:2	20	0.5	67.4	100	18.0 ( <i>R</i> )
13	indene	<b>Mn-2</b>	AcOOH	100:110:1	-20	1	100	94.7 <sup>f</sup>	13.5 (1 <i>R</i> ,2 <i>S</i> )
14	indene	<b>Mn-1</b>	AcOOH	100:110:1	-20	1	100	93.6 <sup>f</sup>	14.9 (1 <i>S</i> ,2 <i>R</i> )
15	indene	<b>Mn-2</b>	HCO <sub>3</sub> H	100:125:1	0	2	13.1	80.1 <sup>b</sup>	nd
16	indene	<b>Mn-2</b>	<i>m</i> -CPBA	100:125:1	0	2	100	96.1 <sup>b</sup>	13.0 (1 <i>R</i> ,2 <i>S</i> )
17	indene	<b>Mn-2</b>	<i>t</i> BuOOH	100:110:1	0	3.5	49.1	46.4 <sup>c</sup>	15.0 (1 <i>R</i> ,2 <i>S</i> )
18	indene	<b>Mn-2</b>	CHP	100:110:1	0	3.5	42.0	83.3 <sup>d</sup>	11.0 (1 <i>R</i> ,2 <i>S</i> )
19	indene	<b>Mn-2</b>	PhIO	100:110:2	20	0.75	57.8	100	24.0 (1 <i>R</i> ,2 <i>S</i> )
20	indene	<b>Mn-2</b>	MesIO	100:110:1	20	1.33	37.1	100	10.5 (1 <i>R</i> ,2 <i>S</i> )
21	1-octene	<b>Mn-2</b>	AcOOH	200:250:1	0	3	94.7	100	4.0 ( <i>R</i> )
22	1-octene	<b>Mn-2</b>	<i>t</i> BuOOH	100:110:1	0	3.5	75.0	89.3 <sup>b</sup>	20.0 ( <i>R</i> )
23	1-octene	<b>Mn-2</b>	PhIO	100:110:2	20	0.75	59.1	100	6.2 ( <i>R</i> )
24	1-octene	<b>Mn-2</b>	MesIO	100:110:1	20	4	49.4	100	4.0 ( <i>R</i> )
25	dbpcn	<b>Mn-2</b>	AcOOH	100:110:1	0	1	95.5	71.4 <sup>f</sup>	40.3 (3 <i>R</i> ,4 <i>R</i> )
26	dbpcn	<b>Mn-2</b>	PhIO	100:110:1	0	2	39.7	100	58.0 (3 <i>R</i> ,4 <i>R</i> )
27	dbpcn	<b>Mn-2</b>	PhIO	40:44:1	-20	3	80.0	100	57.3 (3 <i>R</i> ,4 <i>R</i> )
28	dbpcn	<b>Mn-2</b>	AcOOH	100:110:1	-20	0.5	100	62.5 <sup>f</sup>	60.3 (3 <i>R</i> ,4 <i>R</i> )
29	dbpcn	<b>Mn-2</b>	AcOOH	100:110:1	-20	0.17	100	84.4 <sup>f</sup>	61.2 (3 <i>R</i> ,4 <i>R</i> )
30	dbpcn	<b>Mn-2</b>	AcOOH	100:110:1	-30	0.17	90.8	91.9 <sup>f</sup>	78.7 (3 <i>R</i> ,4 <i>R</i> )
31	dbpcn	<b>Mn-2<sup>e</sup></b>	AcOOH	100:110:1	-30	0.17	98.3	95.9 <sup>f</sup>	79.3 (3 <i>R</i> ,4 <i>R</i> )
32	dbpcn	<b>Mn-1</b>	AcOOH	100:110:1	-30	0.17	97.2	92.9 <sup>f</sup>	77.5 (3 <i>S</i> ,4 <i>S</i> )

<sup>a</sup>In acetonitrile. <sup>b</sup>Side product: 1,2-diol. <sup>c</sup>Side products: 5.9% 1,2-diol + 20.4% allylic alcohol. <sup>d</sup>Side product: allylic alcohol. <sup>e</sup>Reaction performed under an argon atmosphere. <sup>f</sup>Side product: products of the epoxide ring opening with AcOH were detected.

replacement of AcOOH with performic acid led to a slightly lower ee in styrene epoxidations (entry 4). In contrast, *m*-CPBA as the oxidant led to a much lower enantioselection (entry 5). *t*BuOOH was found to be a poorer oxidant: significant conversion was attained only after 3.5 h at 0 °C (entries 6 and 7). The use of cumyl hydroperoxide (CHP) and iodosylarenes led to lower ee's (entries 8 and 9–12).

Quite remarkable is the observed effect of the oxidant on the epoxidation enantioselectivity. This effect, rather insignificant for PhIO and MesIO (14.5 and 18% ee at 20 °C), is more pronounced for *t*BuOOH and CHP (27% and 18% ee at 0 °C) and HCOOH and *m*-CPBA (29% and

11% ee at 0 °C). This difference is also well seen in indene epoxidations (entries 13–20). When using *t*BuOOH for indene epoxidation, a significant amount of the allylic oxidation product was found. The epoxidation of 1-octene demonstrated a poorer enantioselectivity, again with different ee's for different oxidants (entries 21–24).

We found another alkene, 2,2-dimethyl-2*H*-1-benzopyran-6-carbonitrile (dbpcn), to be a more suitable substrate for the asymmetric epoxidation over **Mn-2**. Indeed, the oxidation of dbpcn with AcOOH and PhIO at 0 °C resulted in epoxide formation in 40.3 and 58.0% ee, respectively (entries 25 and 26). Interestingly, lowering the temperature to -20 °C led to a much higher



enantioselectivity in the case of AcOOH (cf. entries 25 and 28–31), while it had a negligible effect in the case of PhIO (entries 26 and 27). In the AcOOH epoxidations, significant amounts of the epoxide ring-opening products (with AcOH) were found in the reaction mixture; that could be partially avoided by shortening the reaction time and lowering the temperature (cf. entries 28–32). Further cooling also led to even higher enantioselectivity, with the highest value of 77.5–79.3% ee being achieved for both enantiomers of the catalyst (**Mn-1** and **Mn-2**), with opposite epoxide configurations (entries 30–32). The presence of oxygen was found to have negligible effect on the catalytic epoxidation: control experiments performed under an argon atmosphere showed similar yields and ee's (cf. entries 6 and 7, 11 and 12, and 30 and 31).

Thus, on the basis of the epoxidation results, one can see that styrene and, particularly, dbpcn, are the best substrates for epoxidation over **Mn-2** with peracetic (and performic) acid. The observed dependence of the epoxidation enantioselectivities on the nature of the oxidants evidences the presence of the oxidant molecule in the structures of the oxygenating intermediates, thus suggesting the composition of the active intermediates as  $[(\text{ROO})\text{Mn}(\text{L})]^{m+}$  ( $\text{R} = \text{acyl or alkyl}$ ) and  $[(\text{ArIO})\text{Mn}(\text{L})]^{m+}$ . The valence state of manganese and the nature of ligands ("L") in the intermediates will be discussed below.

To disclose a possible effect of the counteranion<sup>11</sup> on the catalytic reaction, styrene epoxidations with the in situ prepared catalysts were undertaken. The counteranion effect observed was negligible. On the contrary, a small structural change in the ligand framework (replacement of N–Me with N–H moieties) led to the reversal of the absolute configuration of the epoxide and a dramatic enantioselectivity drop. Interestingly, the change of the reaction solvent altered the reaction selectivity. In particular, in methanol, the epoxide ring-opening products prevailed. These data, along with the results of sulfide oxidation over **Mn-2**, can be found in the Supporting Information (SI; Tables S2–S4).

**High-Valence Manganese Species in AcOOH- and tBuOOH-Based Systems.** Encouraged by the earlier experience in the EPR monitoring of the high-valence manganese intermediates in Mn(salen)-catalyzed epoxidations,<sup>4</sup> we have undertaken an EPR study of the present catalytic system. The EPR spectrum of the frozen solution of the starting catalyst **Mn-2** dissolved in  $\text{CH}_3\text{CN}$  is presented in Figure 1a. The lines have been found to be rather broad; however, one can distinguish the main spectral features at  $g = 5.2, 3.1, 2.0,$  and  $1.44$ . The spectrum is typical for  $S = 5/2$   $\text{Mn}^{\text{II}}$  and is similar to those for structurally similar manganese(II) aminopyridine complexes<sup>12a</sup> and manganese-containing enzyme MnMndD.<sup>12b</sup>

One can see that, after the addition of 1.5 equiv of peracetic acid at  $-30^\circ\text{C}$  in the absence of substrates, the starting manganese(II) complex disappears within less than 2 min (Figure 1b). At the same time, the sample, originally colorless, turns brown. One can also detect the appearance of multiline spectra at  $g = 2.00$  (the nature of this will be discussed later) as well as the formation of at least two mononuclear manganese(IV) species: a broad

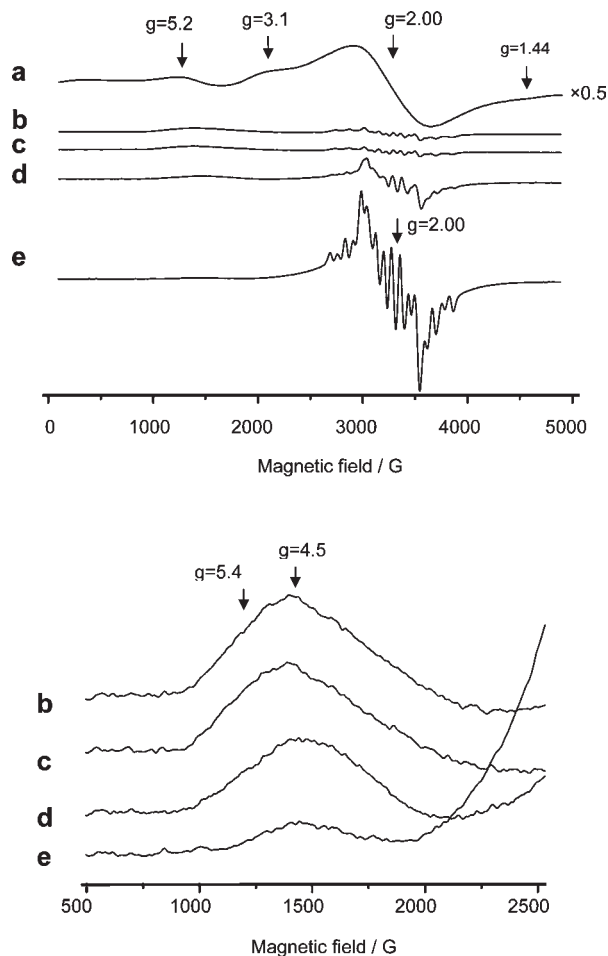


**Figure 1.** X-band EPR spectra (77 K,  $\text{CH}_3\text{CN}$ ) of (a) frozen solution (0.01 M) of complex **Mn-2**, (b) the same solution after the addition of 1.5 equiv of AcOOH at  $-30^\circ\text{C}$  and 2 min of storage at this temperature, (c) the same solution after the addition of 3 equiv of styrene at  $-30^\circ\text{C}$  and 5 min of storage at this temperature, (d) the same solution stored for 15 min at  $20^\circ\text{C}$ , and (e) the same solution stored overnight at  $20^\circ\text{C}$ . In the bottom, the low-field region is presented in more detail.

signal at  $g = 4.5$  with a shoulder at  $g = 5.4$ .<sup>13</sup> The shoulder at  $g = 5.4$  belongs to a less stable species and disappears after the addition of a substrate (styrene) and a gradual warming from  $-30^\circ\text{C}$  to room temperature. The remaining peak at  $g = 4.5$  is more stable and disappears only after storing for hours at room temperature (Figure 1c–e). The picture observed after storage of the sample at room temperature ( $g = 2.0$ ; Figure 1e) is, in fact, the 6-line spectrum of  $\text{Mn}^{\text{II}}(\text{OTf})_2$  (see the SI) superimposed over a 16-line spectrum of the mixed-valence binuclear manganese(III)/manganese(IV) species (see below).

In principle, one could expect that the manganese(IV) species formed after the interaction of **Mn-2** with AcOOH are those responsible for oxygen transfer to the alkene. However, our observations do not support this hypothesis. Indeed, the reactivity pattern of the manganese(IV)

(12) (a) Hureau, C.; Blondin, G.; Charlot, M. F.; Philouze, C.; Nierlich, M.; Césario, M.; Anxolabéhère-Mallart, E. *Inorg. Chem.* **2005**, *44*, 3669–3683. (b) Gunderson, W. A.; Zatsman, A. I.; Emerson, J. P.; Farquhar, E. R.; Que, L., Jr.; Lipscomb, J. D.; Hendrich, M. P. *J. Am. Chem. Soc.* **2008**, *130*, 14465–14467.

(13) Mononuclear manganese(IV) complexes with  $D > h\nu$  display a stronger feature at  $g = 4-6$  and a weaker one at  $g = 2$ .<sup>4,5a,14</sup>

(11) Shoumacker, S.; Hamelin, O.; Pécaut, J.; Fontecave, M. *Inorg. Chem.* **2003**, *42*, 8110–8116.

species (which disappear in the presence of styrene within hours at room temperature) is inconsistent with that observed in the catalytic reactions (complete conversion of styrene within minutes at  $-30$  to  $0$  °C). Furthermore, when the products formed in the sample of Figure 1e were analyzed by chiral high-performance liquid chromatography (HPLC), only trace amounts of styrene epoxide (epoxide yield less than 1% based on AcOOH added) along with a number of unidentified side products and, predominantly, recovered styrene were observed. We suppose that the formation of side products could be caused by some of the manganese(IV) species: indeed, oxomanganese(IV) porphyrin<sup>15</sup> and salen<sup>4b,5a,14b</sup> complexes are known to react with alkenes to yield radical-type oxidation products.

The experiment in Figure 1 was conducted in CH<sub>3</sub>CN because the latter was used as a solvent in the catalytic reactions. However, the lines in the spectra in frozen CH<sub>3</sub>CN were rather broad, and in further studies, acetonitrile was replaced with a 3:2 (v/v) CH<sub>3</sub>CN/CHCl<sub>3</sub> mixture. Although one could expect that CHCl<sub>3</sub> might complicate the chemical behavior of the system due to the formation of Cl• radicals, no evidence for that was observed in our experiments: the same manganese complex/oxidant combinations displayed the same reaction behavior irrespective of the solvent composition (for an example, see the SI).

The spectrum of **Mn-2** in CH<sub>3</sub>CN/CHCl<sub>3</sub> is presented in Figure 2a. One can see multiple features, some with resolved hyperfine splitting, at  $g = 9.5$  ( $a_{\text{Mn}} = 82.7$  G,  $I = 5/2$ ), 4.8 and 4.14 ( $a_{\text{Mn}} \approx 89$  G,  $I = 5/2$ ), 3.14, 2.34, and 2.00 ( $a_{\text{Mn}} \approx 82$  G,  $I = 5/2$ , poorly resolved), and 1.44.

*tert*-Butyl hydroperoxide (*t*BuOOH) appeared to be less reactive toward **Mn-2** (Figure 2). Indeed, while AcOOH converted **Mn-2** into manganese(IV) within 2 min at  $-30$  °C, the complete disappearance of the initial manganese(II) spectrum occurred only after storage of the sample for 17 min at  $0$  °C in the presence of *t*BuOOH (Figure 2a–c). This interaction was accompanied by a color change (from colorless to brown), and a spectrum displaying a feature at  $g = 4.4$ – $4.45$  (marked as  $g = 4.4$ ) and again the 16-line signal at  $g = 2.00$  were observed. The 16-line spectrum at  $g = 2$  has been assigned to an antiferromagnetically coupled ( $S = 1/2$ ) [(2)**Mn**<sup>III</sup>( $\mu$ -O)<sub>2</sub>-**Mn**<sup>IV</sup>(2)]<sup>3+</sup> mixed-valence complex analogous to those previously reported for Mn(salen),<sup>14b</sup> manganese aminopyridine,<sup>12a,16a,b</sup> and manganese bipyridine<sup>16c</sup> complexes (for the simulation of the 16-line spectrum, see the SI).

The signal at  $g = 4.4$  belongs to a manganese(IV) complex similar to that responsible for the EPR feature at  $g = 4.5$  in the **Mn-2**/AcOOH system (Figure 1) and displays a similar reactivity pattern toward styrene: (1) it disappears only after  $>1$  h of storage at room temperature in the presence of styrene and (2) it does not lead to the formation of styrene epoxide (the HPLC analysis detected only trace amounts of styrene epoxide in the sample of Figure 2e, along with small amounts of unidentified products and recovered styrene). The mixed-

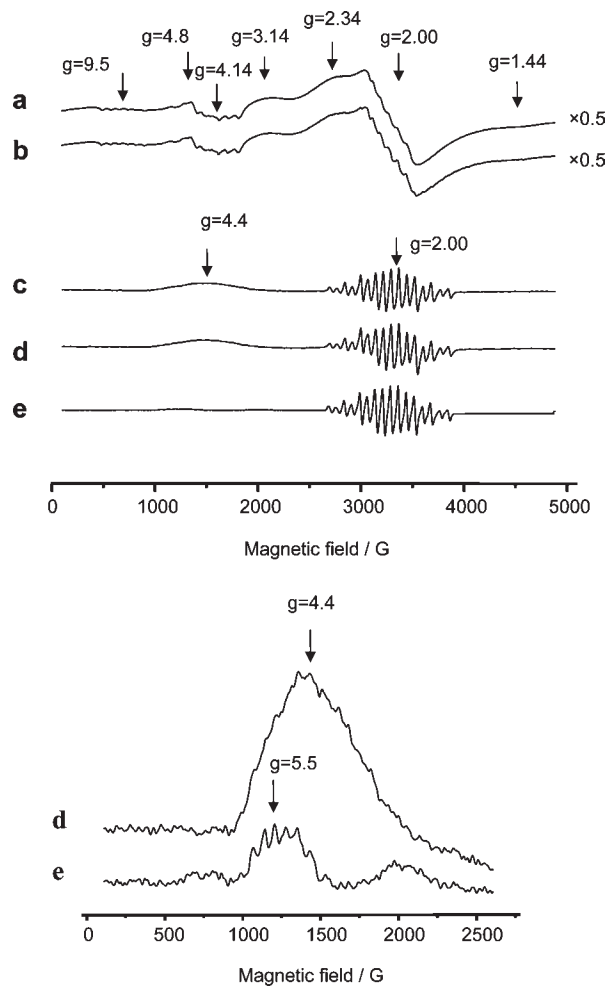


**Figure 2.** X-band EPR spectra (77 K, CH<sub>3</sub>CN:CHCl<sub>3</sub> = 3:2) of (a) frozen solution (0.01 M) of complex **Mn-2**, (b) the same solution after the addition of 1 equiv of *t*BuOOH at  $-10$  °C and 10 min of storage at this temperature, (c) the same solution after 17 min of storage at  $0$  °C, (d) the same solution after the addition of 3 equiv of styrene at  $0$  °C and 30 min of storage at this temperature, and (e) the same solution stored for  $>1$  h at  $+20$  °C. Lower traces represent the low-field region of spectra d and e, respectively.

valence [(2)**Mn**<sup>III</sup>( $\mu$ -O)<sub>2</sub>**Mn**<sup>IV</sup>(2)]<sup>3+</sup> complex showed no activity toward styrene: the intensity of the 16-line spectrum mounted in the course of the experiment (cf. Figure 2b–e). Remarkably, a small amount of a new manganese(IV) species (a signal at  $g = 5.5$  with a partially resolved hyperfine splitting from <sup>55</sup>Mn;  $a_{\text{Mn}} = 72$  G; Figure 2e) remained after the disappearance of the  $g = 4.4$  one, thus again demonstrating inactivity toward styrene. We conclude that none of the observed high-valence manganese species themselves are likely to be the oxygen-transferring intermediates.

A question arises about the nature of the manganese(IV) species that appear in the **Mn-2**/AcOOH and **Mn-2**/*t*BuOOH systems (at  $g = 4.5$  and  $4.4$ , respectively). We believe that those signals belong to the same [O=**Mn**<sup>IV</sup>(2)]<sup>2+</sup> species, with the marginal difference in the apparent  $g$ -factor

(14) (a) Pal, S.; Ghosh, P.; Chakravorty, A. *Inorg. Chem.* **1985**, *24*, 3704–3706. (b) Bryliakov, K. P.; Kholdeeva, O. A.; Vanina, M. P.; Talsi, E. P. *J. Mol. Catal. A: Chem.* **2002**, *178*, 47–53.

(15) (a) Groves, J. T.; Stern, M. K. *J. Am. Chem. Soc.* **1988**, *110*, 8628–8638. (b) Groves, J. T.; Watanabe, Y. *Inorg. Chem.* **1986**, *25*, 4808–4810.

(16) (a) Groni, S.; Dorlet, P.; Blain, G.; Bourcier, S.; Guillot, R.; Anxolabéhère-Mallart, E. *Inorg. Chem.* **2008**, *47*, 3166–3172. (b) Groni, S.; Hureau, C.; Guillot, R.; Blondin, G.; Blain, G.; Anxolabéhère-Mallart, E. *Inorg. Chem.* **2008**, *47*, 11783–11797. (c) Weare, W. W.; Pushkar, Y.; Yachandra, V. K.; Frei, H. *J. Am. Chem. Soc.* **2008**, *130*, 11355–11363.

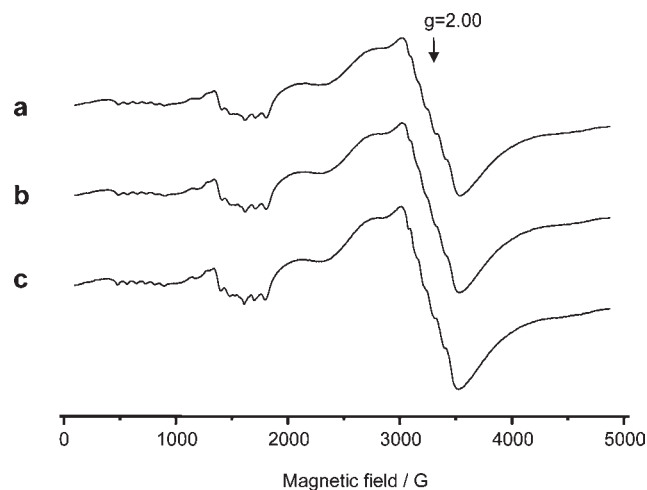


**Figure 3.** X-band EPR spectra (77 K,  $\text{CH}_3\text{CN}:\text{CHCl}_3 = 3:2$ ) of (a) a frozen solution (0.01 M) of complex **Mn-2**, (b) the same solution after the addition of 3 equiv of styrene and then 1 equiv of AcOOH at  $-35^\circ\text{C}$ , and (c) the same solution stored for 5 min at  $0^\circ\text{C}$ .

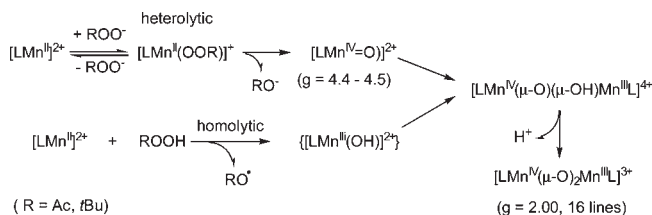
position being caused by the different axial ligands present (e.g.,  $\text{AcO}^-$  or  $t\text{BuOH}$ ). Similar oxomanganese(IV) complexes were previously detected in Jacobsen and Mukaiyama systems (oxomanganese(IV) salen)<sup>4b,5a,14b,17</sup> and porphyrin catalyst systems (oxomanganese(IV) porphyrin).<sup>15</sup> This assignment is corroborated by the observed reactivity pattern of  $[\text{O}=\text{Mn}^{\text{IV}}(\mathbf{2})]^{2+}$  and the presence of the same species in the **Mn-2**/ArIO systems (see below).

For comparison, we have monitored the reactions in the system **Mn-2**/styrene after the addition of AcOOH (Figure 3). Virtually no evolution of spectra has been detected (and no brown color observed). As expected, a nearly quantitative yield of styrene epoxide (with 36% ee) based on AcOOH has been found by the chiral HPLC analysis of the sample in Figure 3c. The observed behavior could be rationalized in two ways: either (1) no high-valence manganese complexes are formed in the presence of a substrate (which means that **Mn-2** itself catalyzes the epoxidation without a change of the oxidation state) or (2) a small amount of high-valence manganese species that is highly catalytically active is formed, so that all oxidant is rapidly consumed to yield the enantioenriched epoxide. These alternatives will be considered below.

Thus, manganese complexes in higher oxidation states are particularly unlikely to be responsible for the enantioselective epoxidation of alkenes via the oxygen-rebound mechanism. To describe the processes occurring in these systems in the absence of substrate, the following reaction scheme is proposed based on the obtained and literature data (Scheme 2).

Apparently, **Mn-2**, as a transition-metal complex, can catalyze both hetero- and homolytic peroxide O–O bond cleavage.<sup>18</sup> At the first stage, formation of the  $[(\mathbf{2})\text{Mn}^{\text{II}}(\text{OOR})]^+$  complex can be expected followed by further conversion to the  $[(\mathbf{2})\text{Mn}^{\text{IV}}=\text{O}]^{2+}$  one.<sup>8a</sup> On the other

**Scheme 2.** Possible Reactions in the Systems **Mn-2**/AcOOH and **Mn-2**/ $t\text{BuOOH}$



part, homolytic peroxide cleavage would give the  $[(\mathbf{2})\text{Mn}^{\text{III}}(\text{OH})]^{2+}$  complex,<sup>19</sup> which, upon reaction with the  $[(\mathbf{2})\text{Mn}^{\text{IV}}=\text{O}]^{2+}$  complex, could lead to the apparent thermodynamic sink of this and related<sup>12a,14b,16a,16b</sup> systems: the mixed-valence binuclear complex  $[(\mathbf{2})\text{Mn}^{\text{IV}}(\mu\text{-O})_2\text{Mn}^{\text{III}}(\mathbf{2})]^{3+}$  (Scheme 2). Otherwise, the formation of manganese(III) necessary for association with the  $\text{Mn}^{\text{III}}\text{Mn}^{\text{IV}}$  dimer could result from a one-electron reduction of  $[(\mathbf{2})\text{Mn}^{\text{IV}}=\text{O}]^{2+}$ .

Trying to get further proof for this scheme, we have undertaken a  $^2\text{H}$  NMR spectroscopic study of the system **Mn-2**/ $t\text{BuOOH}-d_9$ <sup>20</sup> at low temperatures ( $-40$  to  $-10^\circ\text{C}$ ).<sup>21</sup> No  $^2\text{H}$  peaks attributable to the manganese(III) or (IV)  $\text{OOC}(\text{CD}_3)_3$  group were detected.<sup>22</sup> At the same time, we know that, once formed, manganese(IV) and manganese(III)/manganese(IV) complexes disappear in the presence of styrene rather slowly and lead mainly to side products rather than styrene oxide. These results could be interpreted in terms of formation of the manganese(II) alkyl- or acylperoxo reactive species.<sup>23</sup> On the other hand, they do not rule out the formation of a rather small concentration of a catalytically active high-valence manganese complex with the oxidant. These alternatives are in agreement with the epoxidation results, which evidence that the peracid (or alkyl hydroperoxide) molecule is incorporated in the structure of the oxygenating intermediate, and the bulkiness of the alkyl- or acylperoxo moiety affects the epoxidation stereoselectivity. This is also confirmed by the isotopic labeling data of Nam and co-workers, who reported no apparent  $^{18}\text{O}$  incorporation from  $\text{H}_2^{18}\text{O}$  in the course of oxidations

(19) We assume the possibility of the existence of the elusive manganese(III) species, although there is no direct proof for its formation. Apparently, its concentration might be too low to be reliably detected by  $^1\text{H}$  NMR or EPR spectroscopy or the electron-spin relaxation is too slow, leading to a broadening of the  $^1\text{H}$  NMR resonances.

(20) A similar technique was used to detect iron(III) alkylperoxo complexes: Sobolev, A. P.; Babushkin, D. E.; Talsi, E. P. *J. Mol. Catal. A: Chem.* **2000**, *159*, 233–245.

(21) The interaction was monitored by  $^2\text{H}$  NMR until the disappearance of the starting **Mn-2** and  $[(\mathbf{2})\text{Mn}^{\text{IV}}=\text{O}]^{2+}$ , so that only the manganese(III)/manganese(IV) binuclear complex remained in the sample.

(22) Only manganese(III) and manganese(IV) complexes might (in principle) be detected by NMR spectroscopy,<sup>4,17</sup> whereas manganese(II) cannot be observable because of the slower electron-spin relaxation. Therefore, only manganese(II) alkylperoxo complexes are expected to be present in relatively high concentrations in the system **Mn-2**/ $t\text{BuOOH}-d_9$ .

(23) One might also consider the possibility of low-spin (diamagnetic) oxomanganese(V) intermediates, which have been previously discussed in the literature for manganese-catalyzed oxidations.<sup>3–5</sup> However, in a series of variable-temperature measurements on **Mn-2** with AcOOH,  $t\text{BuOOH}$ , and PhIO as oxidants, no diamagnetic signals that could be ascribed to the  $\text{Mn}^{\text{V}}=\text{O}$  species were detected. Moreover, the isotopic labeling data of Nam and co-workers and our catalytic data run counter to the hypothesis of the oxomanganese(V) intermediate.

(17) Kurahashi, T.; Kikuchi, A.; Tosha, T.; Shiro, Y.; Kitagawa, T.; Fujii, H. *Inorg. Chem.* **2008**, *47*, 1674–1686.

(18) (a) Balasubramanian, P. N.; Bruce, T. C. *Proc. Natl. Acad. Sci. U.S.A.* **1987**, *84*, 1734–1738. (b) Jensen, M. P.; Lange, S. J.; Mehn, M. P.; Que, E. L.; Que, L., Jr. *J. Am. Chem. Soc.* **2003**, *125*, 2113–2128. (c) Kozlov, Y. N.; Nizova, G. V.; Shul'pin, G. B. *J. Phys. Org. Chem.* **2008**, *21*, 119–126.



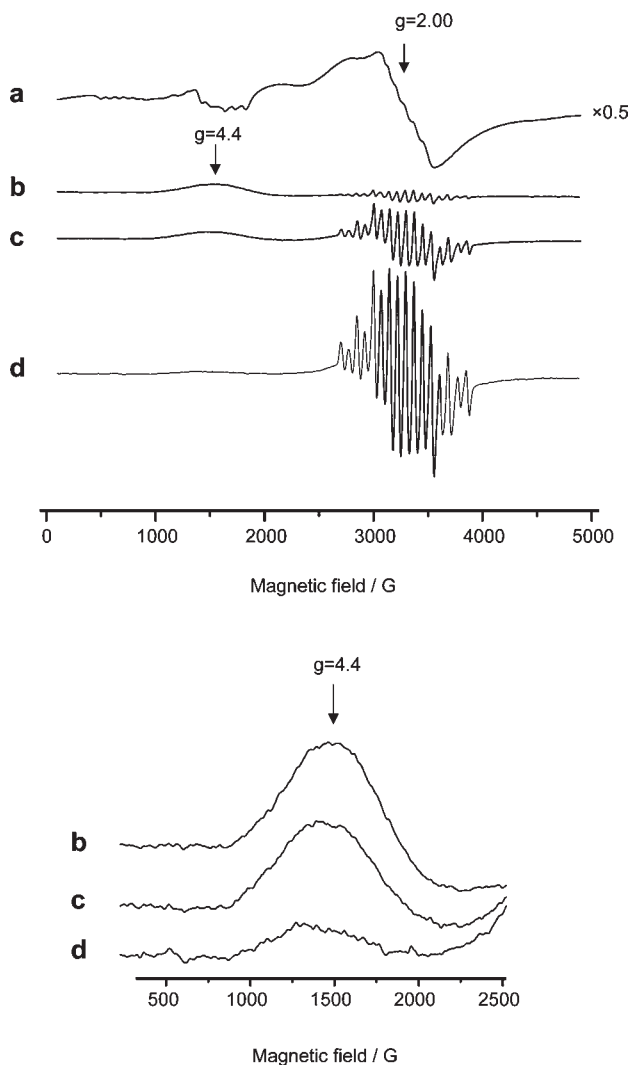


**Figure 4.** X-band EPR spectra (77 K,  $\text{CH}_3\text{CN}:\text{CHCl}_3 = 3:2$ ) of (a) a frozen solution (0.01 M) of complex **Mn-2**, (b) the same solution after the addition of 2.5 equiv of MesIO at  $-10\text{ }^\circ\text{C}$  and shaking of the sample for 5 min at  $<-10\text{ }^\circ\text{C}$ , (c) a sample of that in part b after the addition of 3 equiv of styrene and storage for 15 min at  $10\text{ }^\circ\text{C}$ , and (d) the same solution stored for an additional 30 min at  $20\text{ }^\circ\text{C}$ . Lower traces represent the low-field region of spectra d–f.

with AcOOH catalyzed by a similar manganese aminopyridine complex. The latter could be interpreted as evidence that no high-valence oxomanganese species (which is expected to exchange the oxo moiety with  $^{18}\text{O}$ -labeled water) itself acts as the oxygen carrier in the catalytic oxidation.<sup>7a</sup>

Thus, one could conclude that **Mn-2** or some high-valence manganese species derived therefrom acts as a Lewis acid activator of the terminal oxidant. Examples of similar behavior (Lewis acid oxidant activation pathway) have been reported for  $\text{Mn}^{\text{III}}\text{salen}/m\text{-CPBA}$ ,<sup>4b</sup> iron(III) porphyrin/*t*BuOOH,<sup>8b</sup>  $\text{Mn}^{\text{III}}/\text{aldehyde}/\text{O}_2$ ,<sup>8c,d,14b</sup> and other<sup>9,10</sup> catalytic systems.

**High-Valence Manganese Species in ArIO-Based Systems.** The main stages of the interaction of **Mn-2** with MesIO have been monitored by EPR (Figure 4). After the addition of MesIO to the solution of **Mn-2** and vigorous shaking of the sample (maintaining the temperature below  $-10\text{ }^\circ\text{C}$ ), the EPR spectra of the mixed-valence binuclear complexes  $[(2)\text{Mn}^{\text{IV}}(\mu\text{-O})_2\text{Mn}^{\text{III}}(2)]^{3+}$  (16 lines

at  $g = 2$ ; Figure 4b–d) as well as the already known feature at  $g = 4.4$  (Figure 4) were observed. After the addition of styrene and a prolonged (over 0.5 h) storing of the sample at  $20\text{ }^\circ\text{C}$ , the resonance at  $g = 4.4$  almost disappeared (Figure 4e–g). At the same time, the concentration of  $[(2)\text{Mn}^{\text{IV}}(\mu\text{-O})_2\text{Mn}^{\text{III}}(2)]^{3+}$  increased. Chiral HPLC analysis of the sample in Figure 4d revealed trace amounts of unidentified side products and no styrene epoxide, with recovered styrene being the major substance in the mixture. When PhIO was used instead of MesIO, a similar behavior was documented by EPR and chiral HPLC.<sup>24</sup>

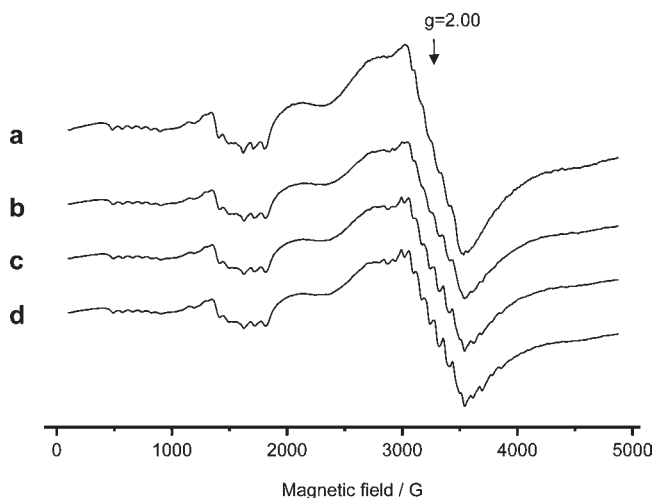
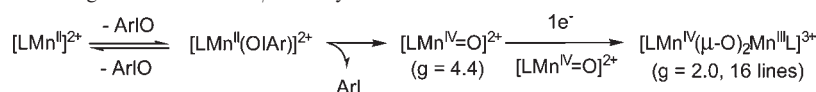
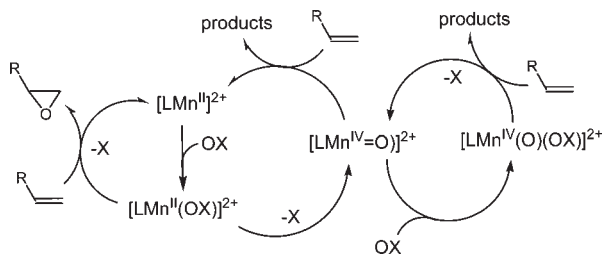
Thus, as for the **Mn-2**/AcOOH and **Mn-2**/*t*BuOOH systems, an oxygen-rebound catalytic mechanism involving oxomanganese(IV) species is unlikely in the **Mn-2**/ArIO systems. The  $[(2)\text{Mn}^{\text{IV}}=\text{O}]^{2+}$  ( $g = 4.4$ ) complex, initially formed upon interaction with ArIO, can only yield the  $[(2)\text{Mn}^{\text{IV}}(\mu\text{-O})_2\text{Mn}^{\text{III}}(2)]^{3+}$  dimers (16-line spectrum at  $g = 2.00$ ) and side products of styrene oxidation. Thus, on the basis of these findings, in the absence of a substrate, one can formulate the reaction scheme given in Scheme 3.

On the contrary, when styrene was added to the sample containing **Mn-2** before the oxidant, manganese(II) was found to prevail in the reaction mixture even after a prolonged shaking with PhIO (Figure 5a–d). Actually, the concentration of **Mn-2** slightly dropped during the first 3 min of interaction with iodobenzene (Figure 5a,b), and a trace amount of the  $[(2)\text{Mn}^{\text{IV}}(\mu\text{-O})_2\text{Mn}^{\text{III}}(2)]^{3+}$  binuclear species was detected after further shaking and storage of the sample at  $0\text{ }^\circ\text{C}$  (Figure 5c,d). However, most of the manganese (over 75%) remained in the form of **Mn-2**. Chiral HPLC analysis of the sample in Figure 5d revealed styrene epoxide as the major reaction product (with nearly quantitative yield), with 27% ee.

**On the Nature of the Oxidizing Species.** We summarize that, basically, two possible reaction pathways could be expected for catalytic oxidation with ArIO (Scheme 4). On the basis of the EPR data, we could rule out the oxygen-rebound pathway because the  $[(2)\text{Mn}^{\text{IV}}=\text{O}]^{2+}$  species (as well as  $[(2)\text{Mn}^{\text{IV}}(\mu\text{-O})_2\text{Mn}^{\text{III}}(2)]^{3+}$ ) proved their inability to epoxidize olefins enantioselectively, and the process enantioselectivity was found to depend on the oxidant used.

The remaining opportunities imply the Lewis acid activation mechanism and are the following: the reaction proceeds (1) via the  $[(2)\text{Mn}^{\text{II}}(\text{oxidant})]^{m+}$  active complex and (2) via the new oxidant of the type  $[(2)\text{O}=\text{Mn}^{\text{IV}}(\text{oxidant})]^{m+}$  similar to that reported for manganese-based oxidation catalysts.<sup>10,23</sup> To discriminate between these opportunities, catalytic experiments with modified addition orders have been performed (Table 3). In particular, a small excess (2–10 equiv) of the oxidant was added to the catalyst solution at the reaction temperature, and the mixture was stirred for some time to accomplish the conversion of **Mn-2** into the high-valence state (mainly to  $[(2)\text{Mn}^{\text{IV}}=\text{O}]^{2+}$ ), which normally takes minutes even

(24) It is worth mentioning that at least 2.5–3.0 equiv of MesIO was required for the complete disappearance of the starting **Mn-2**. This is explained by the presence of methyl groups in MesIO and MesI that could be readily oxidized, thus partially preventing the formation of  $[\text{LMn}^{\text{IV}}=\text{O}]^{2+}$  species. When PhIO was used instead of MesIO, the complete conversion of **Mn-2** to  $[\text{LMn}^{\text{IV}}=\text{O}]^{2+}$  was attained with only 1 equiv of PhIO.

**Scheme 3.** Possible Reactions Taking Place in the Mn-2/PhIO System**Figure 5.** X-band EPR spectra (77 K,  $\text{CH}_3\text{CN}:\text{CHCl}_3 = 3:2$ ) of (a) a frozen solution (0.01 M) of complex **Mn-2**, (b) the same solution after the addition of 3 equiv of styrene and 1 equiv of PhIO at  $0^\circ\text{C}$  and shaking of the sample for 3 min at  $<0^\circ\text{C}$ , (c) the same solution shaken for an additional 3 min at  $<0^\circ\text{C}$ , and (d) the same solution stored for 5 min at  $0^\circ\text{C}$ .**Scheme 4.** Alternative Reaction Pathways for Manganese-Catalyzed Asymmetric Catalytic Epoxidation with Two-Electron Oxidants (OX = Oxygen-Rebound Pathway; Center) and Lewis Acid Oxidant Activation Pathways Involving the Two Types of Oxidants (Rather Similar to the “Second Oxidant”<sup>9</sup> and “Third Oxidant”<sup>10</sup> Left and Right)

at low temperatures (vide supra). During this time, the reaction mixtures turned brown. Then the substrate was added, followed by the rest of the oxidant. It was found that the reactions with modified orders gave rather similar results in terms of both the chemical yield and enantioselectivity (cf. entries 1–3, 4 and 5, 6 and 7, and 8 and 9). For epoxidation of dbpcn, the yield and ee were even higher if all of the catalyst was preoxidized to the  $\text{Mn}^{\text{IV}}$  state (entries 1–3). The observed picture is well consistent with the presence of new oxidants that are most likely the  $[(2)\text{O}=\text{Mn}^{\text{IV}}(\text{OAc})]^{2+}$ ,  $[(2)\text{O}=\text{Mn}^{\text{IV}}(\text{OAlk})]^{2+}$ , or  $[(2)\text{O}=\text{Mn}^{\text{IV}}(\text{OAr})]^{2+}$ , depending on the oxidant used, which are rather similar to the “third oxidant” reported by Goldberg and co-workers.<sup>10a,b</sup> The consensus mechanisms for these cases are presented in Scheme 5.

## Conclusions

Enantioselective alkene oxidation with different oxidants (peroxycarboxylic acids, alkyl hydroperoxides, and iodosylarenes) catalyzed by chiral nonheme aminopyridinyl-manganese(II) complexes have been investigated systemati-

cally for the first time. The above complexes have been shown to efficiently catalyze the enantioselective alkene oxidation to the corresponding epoxides in high yield and, depending on the oxidant, substrate, and reaction temperature, up to 79% ee.

The epoxidation enantioselectivities were found to be strongly dependent on the oxidant (and varied within the following groups of oxidants: performic, peracetic, and *m*-chloroperbenzoic acids; *tert*-butyl and cumyl hydroperoxides; iodosylbenzene and iodosylmesitylene), thus indicating that the terminal oxidant molecule is incorporated in the structure of the oxygenating intermediates.

This conclusion was fully corroborated by the EPR data. The latter revealed that the starting  $[\text{LMn}^{\text{II}}]^{2+}$  catalyst (L is the tetradentate aminopyridine ligand), upon interaction with the two-electron oxidant (either  $\text{AcOOH}$ ,  $\text{AlkOOH}$ , or  $\text{ArIO}$ ) in the absence of substrate converted to the  $[\text{LMn}^{\text{IV}}=\text{O}]^{2+}$  complex (at  $g = 4.4\text{--}4.5$ ) and further to the antiferromagnetically coupled  $[\text{LMn}^{\text{IV}}(\mu\text{-O})_2\text{Mn}^{\text{III}}\text{L}]^{3+}$  dimer ( $S = 1/2$ ,  $g = 2.0$ , and 16 lines). None of these high-valence complexes could be directly involved in the oxygen-rebound-type stereoselective epoxidation step and were shown to contribute to minor olefin oxidation sideways. On the contrary, the  $[\text{LMn}^{\text{IV}}=\text{O}]^{2+}$  species was found to act as a Lewis acid activator of the oxidant (acyl and alkyl hydroperoxide or iodosylarene), thus leading to the new oxidant of composition  $[\text{LMn}^{\text{IV}}=\text{O}(\text{OX})]^{n+}$ , rather similar to the “third oxidant” reported by Goldberg and co-workers.<sup>10a,b</sup> The  $[\text{LMn}^{\text{IV}}=\text{O}(\text{OX})]^{n+}$  intermediate accounts for the predominant oxidation pathway in the nonheme manganese-catalyzed olefin epoxidations. We note that the idea of the “third oxidant” preceded by the findings of Goldberg and co-workers<sup>10a,b</sup> (see also the closely related works of Busch et al.<sup>10c</sup> and Zdilla and Abu-Omar<sup>10d</sup>) is quite distinct from that of the “second oxidant”,<sup>8,9</sup> formed by precoordination of the oxidant to the starting (low-valence) catalyst.

We believe that the potential of manganese(II) aminopyridine catalysts in stereoselective oxidations is far from being exhausted, and appropriate ligand tuning as well as a fortunate choice of the oxidant can further improve the catalyst efficiency and stereoselectivity. Such studies are currently underway in our laboratory.

## Experimental Section

All solvents (analytical grade unless otherwise noted) were used without further purification. Ethyl acetate and hexane (reagent grade) were used for column chromatography without purification.  $\text{H}_2\text{O}_2$  was used as an analytical-grade 30% aqueous solution. Silica gel 40 (0.063–0.200 mm) for column chromatography was purchased from Merck. All other chemicals [diacetoxyiodo(benzene), mesityl iodide, alkenes, sulfides, (*R,R*)-1,2-cyclohexanediamine, (*S,S*)-1,2-cyclohexanediamine, substituted pyridinecarboxaldehydes, and *t*BuOOH (5 M solution in decane)] were commercial reagents. Iodosylbenzene (PhIO),<sup>25</sup> iodosylmesitylene,<sup>9h,i</sup> *t*BuOOH-*d*<sub>9</sub>,<sup>20b</sup>  $\text{AcOOH}$ ,<sup>6</sup> and  $\text{Mn}(\text{SO}_3\text{CF}_3)_2$ <sup>26</sup> were prepared as described.

(25) Piaggio, P.; McMorn, P.; Murphy, D.; Bethell, D.; Bulman Page, P. C.; Hancock, F. E.; Sly, C.; Kerton, O. J.; Hutchings, G. I. *J. Chem. Soc., Perkin Trans. 2* **2000**, 2008–2015.

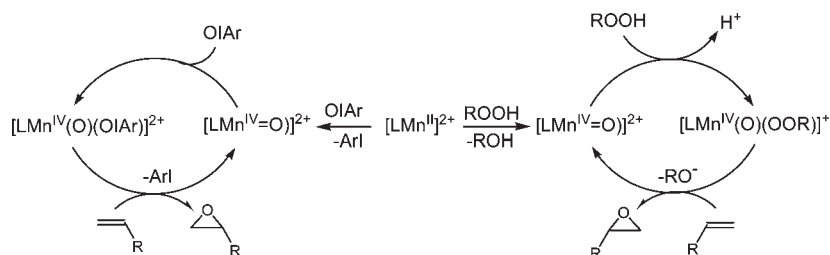


**Table 3.** Enantioselective Oxidation of Alkenes over Manganese Complexes<sup>a</sup>

no.	substrate	complex	oxidant	[alkene]:[O]:[Mn]	T, °C	time, h	conversion, %	epoxide selectivity, %	epoxide ee, % (config)
1	dbpcn	<b>Mn-2</b>	AcOOH	100:110:1	-20	0.17	100	84.4 <sup>b</sup>	61.2 ( <i>R</i> )
2	dbpcn	<b>Mn-2<sup>c</sup></b>	AcOOH	100:110:1	-20	0.17	100	94.9 <sup>b</sup>	72.0 ( <i>R</i> )
3	dbpcn	<b>Mn-2<sup>d</sup></b>	AcOOH	100:110:1	-20	0.17	100	91.9 <sup>b</sup>	72.0 ( <i>R</i> )
4	styrene	<b>Mn-2</b>	MesIO	50:55:1	0	0.67	83.4	100	34.0 ( <i>R</i> )
5	styrene	<b>Mn-2<sup>e</sup></b>	MesIO	50:55:1	0	0.67	70.0	100	30.0 ( <i>R</i> )
6	styrene	<b>Mn-2</b>	AcOOH	100:110:1	-20	2	100	97.6 <sup>g</sup>	35.0 ( <i>R</i> )
7	styrene	<b>Mn-2<sup>f</sup></b>	AcOOH	100:110:1	-20	2	100	97.1 <sup>g</sup>	33.0 ( <i>R</i> )
8	styrene	<b>Mn-2</b>	<i>t</i> BuOOH	100:110:1	0	3.5	50.9	100	24.0 ( <i>R</i> )
9	styrene	<b>Mn-2<sup>h</sup></b>	<i>t</i> BuOOH	100:110:1	0	3.5	43.4	100	22.0 ( <i>R</i> )

<sup>a</sup> Reactions performed in acetonitrile; unless another addition sequence is described, the substrate was added to the solution of the catalyst, followed by the addition of the oxidant. <sup>b</sup> Side products: products of the epoxide ring opening with AcOH. <sup>c</sup> Oxidant (2 equiv) at -20 °C; stirred 5 min; substrate (100 equiv); oxidant (108 equiv). <sup>d</sup> Oxidant (10 equiv) at -20 °C; stirred 5 min; substrate (100 equiv); oxidant (100 equiv). <sup>e</sup> Oxidant (4 equiv) at 0 °C; stirred 5 min; substrate (50 equiv); oxidant (51 equiv). <sup>f</sup> Oxidant (4 equiv) at -20 °C; stirred for 5 min; substrate (100 equiv); oxidant (100 equiv). <sup>g</sup> Side product: 1,2-diol. <sup>h</sup> Oxidant (4 equiv) at 0 °C; stirred for 1 h; substrate (100 equiv); oxidant (100 equiv).

**Scheme 5.** Consensus Catalytic Cycles for the Manganese-Catalyzed Asymmetric Catalytic Epoxidations with ArIO (Left) and Acyl or Alkyl Hydroperoxides (Right)



Other synthetic procedures and spectral data are reported in the SI.

<sup>1</sup>H NMR spectra were measured on a Bruker Avance 400 spectrometer at 400.13 MHz, in 5 mm cylindrical glass tubes. Chemical shifts were referenced to added tetramethylsilane. Typical operation conditions for <sup>1</sup>H NMR measurements were the following: spectral width 8000 Hz, spectrum accumulation frequency 0.4 Hz, number of scans 16–64, radio frequency pulse 2–8 μs, 32–64K data points. <sup>2</sup>H NMR spectra of paramagnetic complex **Mn-2** + *t*BuOOH-*d*<sub>9</sub> were measured on a Bruker Avance 400 spectrometer at 61.422 MHz with the following conditions: spectral width 16000 Hz, spectrum accumulation frequency 5 Hz, number of scans 1024–4096, radio frequency pulse 3 ms, 16K data points. EPR spectra were measured on a Bruker ER200D spectrometer, 9.4 GHz, in 5-mm-o.d. quartz tubes at 77 K.

Enantioselective chromatographic resolution of styrene epoxide enantiomers was performed on a Shimadzu LC-20

chromatograph equipped with a Chiralcel OD-H column (*i*PrOH:*n*-hexane = 1:99, 0.6 mL/min, detection at 216 nm, *t*<sub>S</sub> = 11.6 min, *t*<sub>R</sub> = 12.5 min). Enantioselective chromatographic resolution of dbpcn epoxide enantiomers was performed on a Shimadzu LC-20 chromatograph equipped with a Chiralcel OJ-H column (*i*PrOH:*n*-hexane = 30:70, 1.0 mL/min, detection at 254 nm, *t*<sub>R</sub> = 11 min, *t*<sub>S</sub> = 19 min).

**Acknowledgment.** The authors are grateful to the Russian Foundation for Basic Research (Grant 09-03-00087) for financial support.

**Supporting Information Available:** Extended experimental details, additional epoxidation and sulfoxidation results, simulation of the EPR spectrum of the manganese(III)/manganese(IV) binuclear complex, EPR monitoring of the catalyst/oxidant interactions, and <sup>1</sup>H NMR spectra for some representative reaction mixtures. This material is available free of charge via the Internet at <http://pubs.acs.org>.